JACS
JOURNAL OF THE AMERICAN CHEMICAL SOCIETY
Article
pubs.acs.org/JACS

Shape-Memory and Self-Healing Effects in Mechanosalient Molecular Crystals

Durga Prasad Karothu,[†] James Weston,[†] Israel Tilahun Desta,[†] and Panče Naumov*[,†]

[†]New York University Abu Dhabi, P.O. Box 129188, Abu Dhabi, United Arab Emirates

Supporting Information

ABSTRACT: The thermosalient crystals of terephthalic acid are extraordinarily mechanically compliant and reversibly shape-shift between two forms with different crystal habits. While the transition of form II to form I is spontaneous, the transition of form I to form II is latent and can be triggered by applying local mechanical stress, whereby crystals leap several centimeters in air. This mechanosalient effect (mechanically stimulated motility) is due to sudden release of strain that has accrued in the crystal of form I, which is a metastable structure at ambient conditions. High-speed optical analysis and serial scanning electron microscopy reveal that the mechanical effect is due to rapid reshaping of crystal domains on a millisecond time scale triggered by mechanical stimulation. Mechanically pre-deformed crystals taken over the thermal phase transition exhibit memory effects and partially regain their shape, while cracked, sliced, or otherwise damaged crystals tend to recover their macroscopic integrity by restorative action of intermolecular $\pi-\pi$ interactions in a manner which resembles the behavior of shape-memory and self-healing polymers. These observations provide additional evidence that the thermo-/photo-/mechanosalient effects are macroscopic manifestations of martensitic-type transitions in molecular solids.

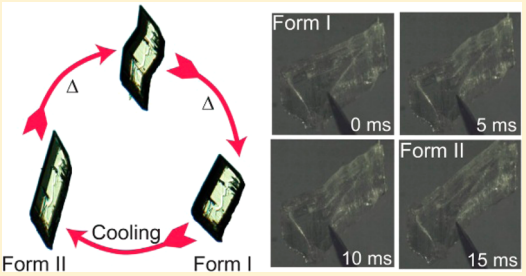

1. INTRODUCTION

Dynamic molecular crystals[1] which can burst,[2−7] jump,[8−19] bend,[20−36] twist,[37−41] or curl[34,42,43] are emerging as efficient macro-/micro-/nanoenergy transducers of heat or light to kinetic energy of mechanical motion. A common feature of these materials is that by virtue of changes in molecular geometry, augmented by the collective action of intermolecular interactions, they can utilize external energy supplied as heat or light to reshape, splinter, explode, and/or move. In the absence of an induction period (a period of latency between the action on the material and the expression of the mechanical response), the shape-shifting of such dynamic solids occurs slowly and simultaneously with the applied stimulus, and single crystals can retain their macroscopic integrity.[1,18,44] By using external force or light, ordered molecular crystals can bend, twist, or coil akin to soft matter such as polymers, elastomers, and liquid crystals in a manner that is atypical for ordered solid states.[45−47] Noteworthy recent examples of such mechanically compliant molecular solids are provided by polyhalogenated benzenes whose crystals, when subjected to localized mechanical stress, can bend to nearly full angle without breaking,[48,49] an organic salt whose crystals can be bent at multiple locations and shaped into zigzag strips,[50] and a tetrafluorobenzene derivative whose acicular crystals can be wrapped multiple times around a cylindrical object.[51] These materials not only bridge the gap between the malleable inorganic materials such as metals or metal alloys and the soft disordered matter such as polymers, but they also provide insight into new, exotic, and hitherto unexplored aspects of the crystal chemistry of molecular solids.

Unlike the slow deformation of crystals such as plastic or elastic bending, rapid actuation attained through the so-called thermosalient and photosalient (crystal leaping) phenomena[1−19] is almost always triggered by a stochastic event and results in disintegrative outcome. Except for a single recently reported case,[52] where when taken over a phase transition crystals of pyroglutamic acid can be recurrently propelled at least 15 times without fracturing, evolution of cracks at defect sites or corners of thermosalient crystals almost invariably results in disintegration by splitting or explosion, rendering such processes unsuitable for practical applications. The efficient coupling between the external stimulus and the elastic energy through their ordered structures could elicit reversible motion on time scales that exceed the typical response times of soft actuators.[53−55] Moreover, their mechanical properties could be the origin of exotic properties such as superelasticity.[50,56,57] However, while faster processes usually result in disintegration, slower processes are less effective in energy transduction. Indeed, the trade-off between the response rate and preservation of crystal integrity currently stands as an unsurmountable impediment toward application of these materials as actuators. Achieving concurrent rapid *and* reversible actuation is at the forefront of the research on dynamic molecular crystals.[58]

In 1994, Davey and Maginn reported[59] that when crystals of polymorph II of terephthalic acid—of which two triclinic forms and one monoclinic form[60] are known—are transformed to

Received: July 18, 2016
Published: September 12, 2016

DOI: 10.1021/jacs.6b07406
J. Am. Chem. Soc. 2016, 138, 13298−13306

polymorph I, they are strongly deformed. The elongated parallelepiped crystals undergo remarkable morphological transformation into a shape which is close to cuboid, whereby they hop off the stage and leap. On the basis of this property and the crystal structure, we have classified terephthalic acid as class III thermosalient solid.[18,61] These materials share as a common motif low-dimensional hydrogen bonded network which can accrue internal strain prior to the phase transition. The transformation is reversible, and when cooled to room temperature the crystals of form I revert to their original elongated shape. Some crystals, however, remain unchanged, and if poked with a needle, they hop off the stage.[59] Plastic deformation under local mechanical stress was reported recently for the diamide of terephthalic acid;[57,62] however, motion was not observed. Our own study of the mechanically stimulated motility of terephthalic acid crystals showed that they are remarkably robust and retain their integrity during the actuation induced by heating as well as by mechanical stimulation. The extraordinary robustness prompted us to investigate the details of molecular (mechanistic) and macroscopic (kinematic) aspects of these phenomena. The results reported here show that the mechanically stimulated crystal motility, for which we propose here the term *mechanosalient effect* (leaping induced by mechanical stimulation), is accompanied by shape-memory and self-healing effects, and we elaborate on the factors which are responsible for these effects.

2. RESULTS AND DISCUSSION

2.1. Salient Effects in Terephthalic Acid Crystals. Crystals of form I terephthalic acid (Figure 1A,B) were obtained as plates or prisms at 423 K, occasionally twinned,

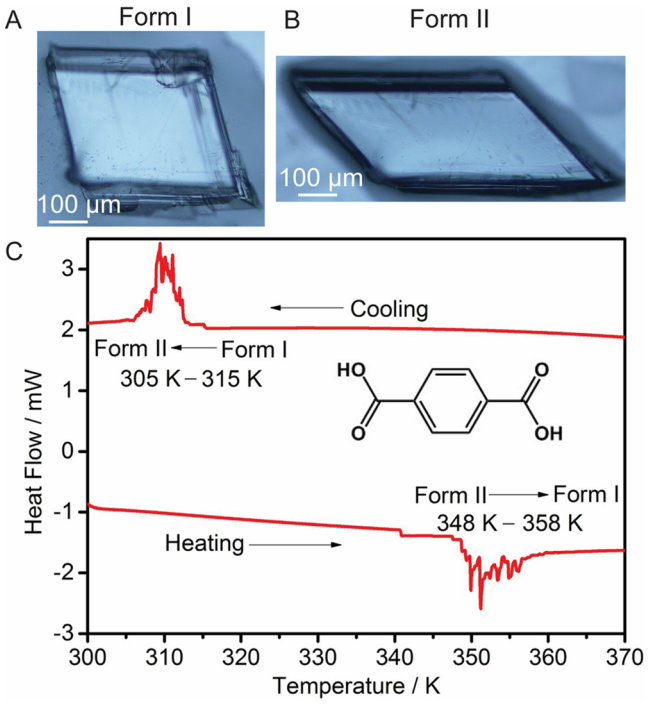

Figure 1. Crystal habits and phase transitions of forms I and II terephthalic acid. (A,B) Typical crystal habits of form I (A) obtained by heating of form II, and of form II (B) obtained by cooling of form I. (C) Thermal effects accompanying the transition between forms II and I recorded by DSC.

from aqueous solution in the presence of *p*-toluic acid as additive, similar to the procedure described in ref 63 (Figure S1). Form II could only be obtained as colorless parallelepiped crystals from acidified aqueous solution at 523 K under hydrothermal conditions (for details of the preparation procedure, see the Experimental Section). X-ray diffraction analysis at 290 K of crystals of both forms reproduced the reported triclinic structures,[63] and the thermal behavior of the two polymorphs was consistent with the results of Davey et al.[59] Differential scanning calorimetry (DSC) confirmed that while form I does not undergo any phase transition on heating to 473 K (Figure S2), form II shows endothermic first-order transition to form I between 348 and 358 K on heating with a "sawtooth" profile of the thermal effects characteristic[61] for a thermosalient transition (Figure 1C). The transition is reversible, and upon cooling form I is converted to form II in the range 305−315 K with a thermal hysteresis of about 43 K (calculated from the average transition temperatures). The thermal analysis alone indicates that form II is more stable than form I at ambient conditions, while form I becomes more stable at high temperature, above the phase transition.

Inspection of the transition by hot-stage microscopy revealed that when heated just above 353 K crystals of form II jump off the hot surface as they are transformed to form I (Movie S1). This self-propulsion is a demonstration of the thermosalient effect,[1,2,4,14,18,19] a phenomenon where crystals acquire momentum and move or burst due to sudden release of the elastic energy accumulated during a first-order phase transition. The details of the reshaping of form II to form I upon transition were inspected using crystals which were fixed by submersion in a minimal amount of oil (Movies S2 and S3). As shown with the stills of the movies in Figure 2A, the originally elongated parallelepiped single crystals visibly shrink and adopt a habit closer to a cuboid without apparent deterioration. As free crystals naturally lie flat on their (010) face, the size of the crystals observed perpendicular to (010) is reduced as much as 26% along their longest side ({100} direction), but only 0.9% along the shorter side.

Many of the transformed crystals of form I recover their original shape after they are cooled to ∼298 K where they transition back to form II (Figure 2B and Movie S4). We noticed, however, that in a few instances crystals of form I retain their shape even after they have been cooled below the transition temperature. The mechanical reconfiguration of these crystals which remain as form I can be triggered by applying local mechanical stress, for example by soft poking with a hard object such as metal needle (Figure 2D and Movie S5). We could not observe specificity in regard to the crystal face on which the pressure was applied; the crystals hopped regardless of the face on which they were stimulated. Visually this mechanically stimulated crystal motility resembles the thermosalient[8−19] and photosalient[4−7] effects. By analogy with these phenomena, we propose here the term *mechanosalient effect* to demarcate mechanically stimulated leaping of crystals. As mentioned above, the thermal data indicate that form I is the more stable phase at high temperature, but becomes metastable phase at room temperature. The local pressure introduces structure perturbation which triggers the phase transition at the point of impact. Immediately following the local transformation, the cooperative effects mediate conversion of larger domains, and eventually the entire crystal is rapidly transformed to form II. If the crystals are restrained from movement (for example, by submersion in viscous liquid), they merely change

DOI: 10.1021/jacs.6b07406
J. Am. Chem. Soc. 2016, 138, 13298−13306

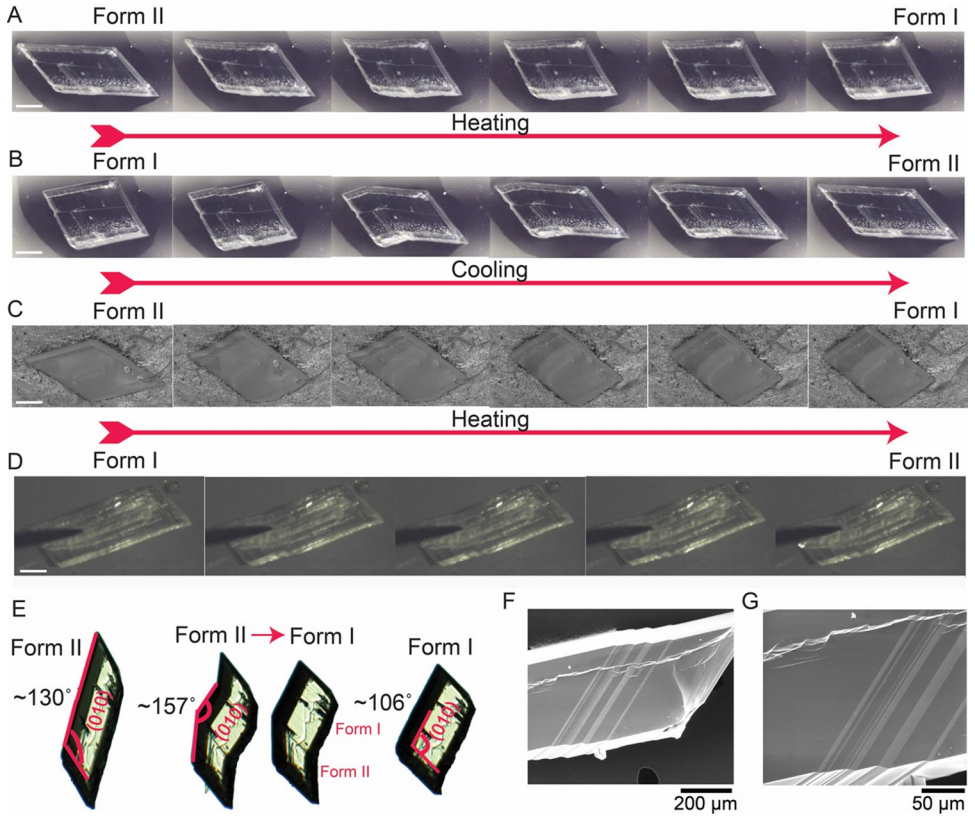

Figure 2. Mechanical reconfiguration of crystals of terephthalic acid during the thermally and mechanically induced phase transitions between forms I and II. (A,B) Snapshots extracted from optical high-speed video recordings of the transition of form II to I (A) and of form I to II (B) (rate: 1500 s^{-1}; see Movies S6 and S7). (C) Snapshots extracted from a movie of the transition of form II to form I recorded using variable-temperature serial hot-stage scanning electron microscopy (Movie S10). (D) Snapshots of the mechanically induced phase transition recorded using optical microscope which triggers the mechanosalient effect (for recordings of the effect, see Movies S11–S15). (E) Changes in angles between the crystal faces during mechanical reconfiguration of a single crystal. (F,G) Scanning electron micrographs showing alternating layers of form II and form I. The length of the scale bars in panels A–D is 100 μm.

their shape. The rapid mechanical reconfiguration of unrestrained crystals releases sufficient elastic energy so that they acquire a momentum and are self-propelled. Inspection of several crystals by optical microscopy revealed that the crystals are remarkably robust; they remained intact and without any apparent defects even after 10 heating–cooling cycles, indicating that the phase transition is highly reconstructive. It is noteworthy that the crystals of form I obtained by crystallization do not undergo mechanosalient effect upon mechanical stimulation.

2.2. Mechanism of Crystal Reshaping. The rapid reshaping of crystals accompanying the phase transitions required inspection of the kinematic details with optical microscope equipped with high-speed camera. Movie S6 contains high-speed recording of the *thermosalient* phase transformation of a single crystal of form II which was constrained from motion by immersion in oil and heated above the phase transition. Movie S7 shows the reverse thermally induced transformation of form I to form II. At a heating rate of 10 K min^{-1}, the entire crystal is transformed within 3 s. The stills in Figure 2A of the thermal transition of form II to form I reveal that the crystal bulk is not converted instantaneously or gradually. Instead, the evolution of the crystal contour with time extracted from the high-speed recordings (Movies S8 and S9) shows clearly that the crystal is transformed by transition of individual parallel crystal domains.

To inspect closer the surface changes that occur during the transition, a serial variable-temperature in situ scanning electron microscopy (SEM) analysis was performed on a single crystal by using a hot stage coupled to an electron microscope (Figure 2C and Movie S10). To record the movie, a crystal was heated at a rate 5 K min^{-1}, and a series of 470 consecutive scans were recorded within 8 min. Figure 2C and the SEM Movie S10 confirm that parallel slabs of the crystal are transformed and reshaped disconcertedly. Similar transformation of individual slabs occurs during the reverse transformation of form I to form II on cooling (Figure 2B and Movie S7).

Movies S11–S15 show similar high-speed recordings of the *mechanosalient* transition. The transformation was induced by poking crystals of form I (obtained by heating of form II and cooling to room temperature) with a metal needle. The mechanically triggered transition is much faster than the thermally induced one; high-speed recordings of the five crystals showed that they were transformed within 30–400 ms after the impact. The thermally and mechanically induced transformations share a common mechanism; however, the overall transition of the crystal occurs on different time scales (Figure 2A,B,D). In either case the transformation is initiated at some of the surface striations on the (010) face of the crystal parallel to its smaller side which correspond to glide planes. The phase front remains straight and progresses very rapidly. The transition is terminated when the advancing front encounters another striation, whereby the transformation of a

DOI: 10.1021/jacs.6b07406
J. Am. Chem. Soc. 2016, 138, 13298–13306

single domain between the two striations is completed. By using atomic force microscopy (AFM), the striations visible on the (010) face of the crystal were identified as stairs between molecular terraces that are at least 35−45 nm high (Figure 3

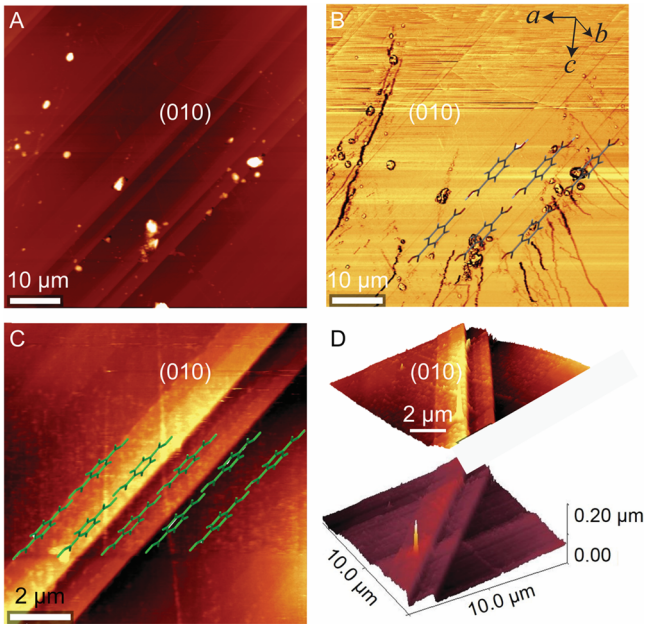

Figure 3. Atomic force microscopy images of the (010) face of form II terephthalic acid recorded in contact mode. (A, B) Topography image (A) and the corresponding phase image (B) of 50 μm × 50 μm area. (C) Topography scan recorded on a 10 μm × 10 μm area. (D) 3D images showing terraces with a step size of 45 nm. The bright regions correspond to the highest points on the surface.

and Figure S3). The orientation of these terraces coincides with the direction of the molecules in the crystal (see section 2.5), and they were identified as slip planes in the crystal interior. In form II, the angle between the slabs and the {100} direction in the crystal of form II is about 130° (Figure 2E). After the transition, the angle between the axes is about 106°. The angle between the non-transformed (parallelepiped, form II) and transformed (close to cuboid, form I) parts is 157°, which corresponds well with the sum of the obtuse angle in form I and the sharp angle of form II (156°).

Regardless of whether the phase transition has been induced thermally or mechanically, initially alternating layers of the converted phase and the parent phase are obtained. The two phases coexist very briefly (milliseconds) during the mechano-salient transition and over longer periods of time (seconds) during the thermosalient transition, before the unconverted phase is converted to the other phase. Alternating layers corresponding to domains of the two phases were observed with crystals of form II which were partially converted to I by heating (Figure 2E), as well as with as-obtained crystals of form II which were partially converted to form I during crystallization (Figure 2F,G). This result confirms that the stable form (II) and the metastable form (I) can coexist at room temperature. The coexistence of alternating thin domains of the two phases also accounts for the slightly curved appearance of the kink of some partially converted bent crystals. The evolution of alternating domains alleviates the overall stress in the crystal, because the interfacial stresses generated at opposite phase boundaries of each domain partially cancel out and result in low differential stress. The conversion of multiple domains in the contact region absorbs the elastic energy and prevents formation of cracks. Consequently, the bulk experiences relatively low strain, and the crystal maintains its microscopic integrity. After a hiatus from the conversion of individual slabs, the remaining untransformed domains are converted, which ultimately results in conversion of a large macroscopic portion or of the entire crystal. The hiatus is much shorter and the overall transition proceeds much faster when the perturbation is induced mechanically relative to the thermal transition. This is due to simultaneous generation of multiple defect sites and initiation of conversion of more domains when local external mechanical stress is applied to the crystal. Consequently, the mechanical stimulation inevitably results in a rapid and strong mechanical effect. On the other hand, the thermally induced transition is slower because the onset is stochastic and initiated spontaneously at glide defects (striations). Gliding of these defects and the realignment of crystal domains imply that interactions between the layers are broken and re-formed in a manner similar to breaking and re-formation of bonds during self-healing processes in polymers.

2.3. Self-Healing and Shape-Memory Phenomena.

The impressive shape recovery and mechanical robustness of the terephthalic acid crystals prompted us to investigate the effect of reshaping by phase transition on the morphology of crystals which were pre-deformed, cracked, damaged, or partially disintegrated. When subject to a pressure on the (010) face in a three-point bending geometry, crystals of form II can be plastically bent without cracking (we note that bending is only possible when the pressure is applied on the (010) surface). This bending occurs due to gliding of parallel layers and re-formation of the interlayer bonds.[49] The deformation is plastic, and at room temperature the bent crystals do not recover their shape. However, as shown in Figure 4A and is even more apparent from Movie S16, when a bent crystal of form II is heated over the phase transition, the slabs realign, the bending angle decreases, and the straight shape of the crystal is partially recovered. This is due to relaxation of the crystal brought about by the transformation of multiple slabs, which become shorter and less skewed after the transition to form I. Surprisingly, the bent shape of the crystal was recovered by cooling to room temperature, where form I reverts to form II. The process can be repeated by heating and cooling, and the crystal can be straightened and bent again.

In another demonstration of the self-healing properties of terephthalic acid crystals, a crystal of form II was pre-defected by pressing it uniformly across the (010) surface by using a metal plate. In response to the application of uniform pressure, the crystal did not bend but cracked into multiple parallel slices instead. When the sliced crystal was taken over the phase transition by heating, the slices slid back and realigned, whereupon the original shape of the crystal was partially recovered (Figure 4B and Movie S17). Even after crystals of form II were severely damaged and cracked by pressing with a needle, as shown in Figure 4C and Movie S18, the slabs retained their ability to realign, and the crystals partially recovered their integrity after heating. This propensity for self-healing is due to re-formation of the intermolecular bonds between the slices which remain close to each other after each of them is converted to form I. This thermally induced shape recovery of a crystal of mechanically deformed molecular solid represents analogy of the shape-memory effects observed with

DOI: 10.1021/jacs.6b07406
J. Am. Chem. Soc. 2016, 138, 13298−13306

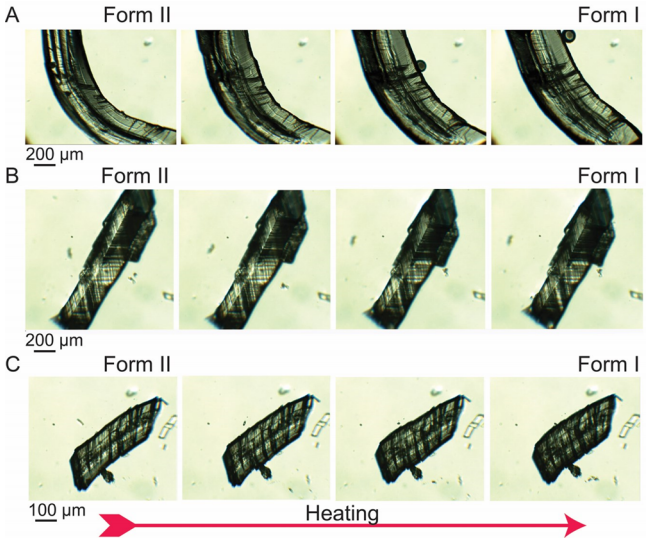

Figure 4. Shape-memory and self-healing behavior of terephthalic acid crystals. (A) A single crystal was deformed by bending in three-point geometry by applying pressure on the (010) face. After heating, the crystal is straightened. After cooling to room temperature, the bent shape is recovered. (B,C) Partial recovery of the crystal integrity after the crystals have been heavily damaged by applying pressure with a flat object (B) or a needle (C). The slices realign after the heating.

metals, metal alloys, and mesophasic materials, such as polymers and elastomers.

2.4. Thermal Expansion Preceding the Thermosalient Effect. As shown in Figure 5, single crystals retain their

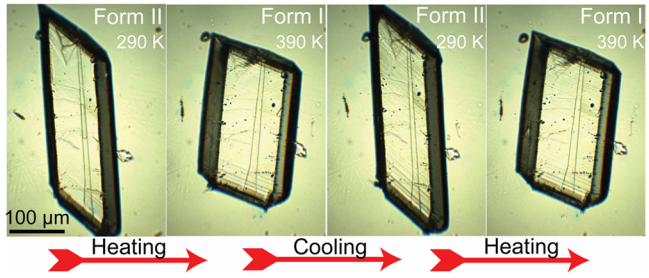

Figure 5. A single crystal of form II terephthalic acid, consecutively taken twice over the phase transition to form I. The crystal does not show any visible deterioration.

integrity when they are repeatedly taken over the phase transition. Variable-temperature in situ X-ray diffraction analysis was performed to determine the structure of the two forms from the same single crystal. A crystal of form II was consecutively taken over the forward transition (II-to-I), the reverse transition (I-to-II), and then again over the forward transition (II-to-I) by controlled heating and cooling on the diffractometer, and diffraction data were collected (Figure S4 shows the actual crystal that was used for X-ray diffraction analysis; Table S1 contains the crystallographic data and structure refinement details).

The transition is reversible and proceeds in a single-crystal-to-single crystal manner. Consistent with almost all thermosalient solids (apart from a couple of spinels[64] and a bipyridyl complex[17,65]), the crystal symmetry during the phase transition (triclinic, $P\bar{1}$) is retained, and the change of the unit cell volume is small (174.7(1) and 177.7(1) Å^3 in forms II and I, respectively). The variation of lattice parameters with temperature in the range 100−360 K in 10 K increments is shown in Figure 6, and the values are listed in Table S2. The unit cell

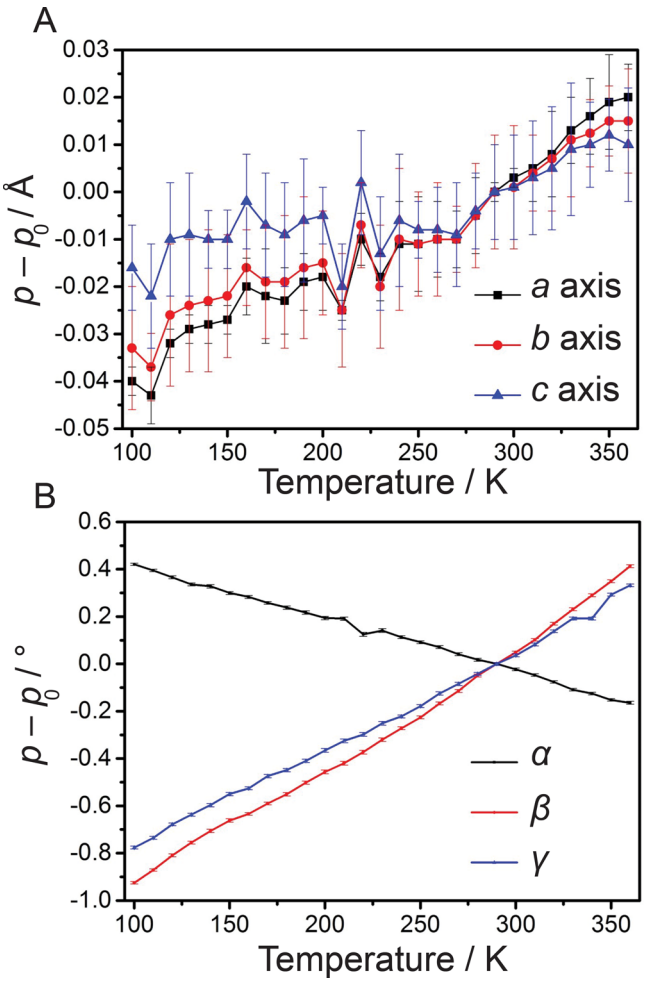

Figure 6. Variation of the unit cell axes (A) and angles (B) of a single crystal of terephthalic acid with temperature. The error bars are calculated as sum of the esd's of p and p_0, where p stands for a generalized unit cell parameter. The parameters p_0 refer to 290 K.

parameters of heated, cooled, and then reheated crystal reflect the transitions between forms II and I (Table S1). As expected, abrupt changes occur during the phase transition on heating. Because the crystal system is triclinic, the expansivities prior to the phase transition were calculated along the principal axes by using the program PAScal[66] (the expansivity indicatrix and the changes of the length of the principle axes with increasing temperature are shown in Figure S5). Along with what has been observed with other systems, the thermal expansion of form II preceding the transition to form I is anisotropic. The minor (X1), medium (X2), and major (X3) principal axes in the crystal are oriented approximately along the {3 −5 8}, {5 8 −1}, and {−8 4 4} directions, respectively. Form II exhibits biaxial positive thermal expansion with coefficients of 4.35 × 10^{-6} K^{-1} and 102.93 × 10^{-6} K^{-1} and small uniaxial negative thermal expansion with coefficient −10.54 × 10^{-6} K^{-1}. The volumetric thermal expansion is 107.29 × 10^{-6} K^{-1}.

2.5. Structural Changes during the Thermosalient Effect. A common motif in the structures of the two polymorphs are infinite tapes of symmetric dimers that are

DOI: 10.1021/jacs.6b07406
J. Am. Chem. Soc. 2016, 138, 13298−13306

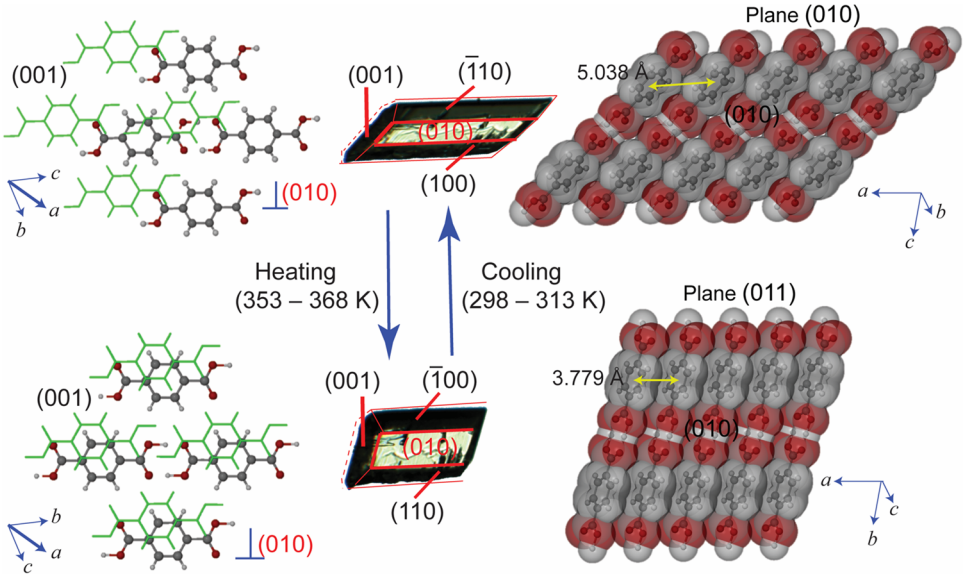

Figure 7. Structure–habit relationships between the two phases of terephthalic acid. The crystal packing is shown with ball-and-stick model on the left and space-filling model on the right. Typical crystal habits with face indices are also shown. Form II is shown on the top, form I on the bottom.

typically observed with *para*-dicarboxylic acids (Figure 7). Each two adjacent molecules within the tapes are bonded with two identical short hydrogen bonds (O···O = 2.625(2) Å and O···H = 1.495(4) Å in form II at 290 K; O···O = 2.626(2) Å and O···H = 1.379(4) Å in form I at 390 K). The molecular tapes are connected by C–H···O interactions (the C···O distance is 3.491(2) Å in form II and 3.566(2) Å in form I), and the tapes from adjacent layers interact with each other through $\pi-\pi$ interactions. The two polymorphs differ in the relative positions of the layers, which brings about different distance between the ring centroids, 5.038(1) and 3.779(1) Å in forms II and I, respectively (Figure 7; see also Figures S6 and S7). In form II the hydrogen-bonded tapes are oriented along the {101} direction, and the sheets are parallel to the (010) plane (Figure S8). The carboxyl group dimers of one layer are positioned approximately above the phenyl rings of the adjacent layer. In form I, on the other hand, the tapes are aligned along the {100} direction, and the sheets are parallel to the (011) plane, which brings the hydrogen-bonded carboxyl groups of one layer approximately above those of an adjacent molecular chain.

We infer about the mechanism of the phase transition and the ensuing morphological changes by comparing the relative arrangement of molecular sheets in the two polymorphs. The slippage angle between the rings in form II is 134° since each phenyl ring is offset from the ring in the neighboring layer and is positioned above a carboxyl group dimer (Figures S6 and S7). When form II is transformed to form I, the adjacent molecular layers slide relative to each other and their relative disposition changes, but they remain stacked (Figure 7). In form I, the phenyl rings from one molecular tape are placed almost atop phenyl rings from the adjacent layer at a slippage angle of 106° between the two phenyl rings. The centroid–centroid distance is reduced from 5.038(1) Å (form II) to 3.779(1) Å (form I).

The delayed transformation of form II to form I, which is required for the thermosalient effect, and the delayed reversal of this transition are due to the capability of these two-dimensional structures for accumulation of strain without transition. The strain is then released upon triggering of the transition at an existing glide plane, as is the case with crystals of form II that are thermally transformed to form I, or by inducing defects with local pressure, as is the case when the crystals of form I are pinched with a needle and transform to form II. Indeed, one of the prerequisites for occurrence of the thermosalient effect in molecular crystals is that they are soft and susceptible to accrual of strain without immediate transformation.[16]

To verify this in the case of terephthalic acid, the mechanical properties of form II crystals were analyzed by nanoindentation. The crystals were indented on their largest face (010) by using the continuous stiffness method to a depth of 1 μm (Figure S9). The uneven appearance of the loading curve reflects the anisotropy of the material, in line with its layered structure. The average hardness of the crystals is 0.33 ± 0.05 GPa, and the elastic modulus is 6.2 ± 0.7 GPa. The relatively high elastic modulus is in line with the restorative propensity of crystals of form II upon mechanical deformation. The indents were examined using SEM and AFM. The topography images (Figure S10) show the depression of the indents with increasing loads. The microscopic cracks are predominantly generated parallel to the sheets on (010) plane, along with the striations observed on the surface of the crystal and follow the direction of the molecular tapes.

3. CONCLUSIONS

The thermosalient (and possibly also the photosalient) effects where crystals move in response to a structural phase transition have been recently identified as organic-based analogues of the martensitic transitions that are known for inorganic materials.[19] These conclusions are in line with the early studies of Jones et al.[67,68] who have provided convincing evidence that molecular solids can undergo martensitic phase transitions. The thermosalient crystals are generally soft and can accrue stress up to a point where the stress is rapidly released as elastic energy of the evolving cracks, whereby crystals splinter, and part of the energy is converted to kinetic energy of motion of the crystal or the crystal debris.

Here, in the case of terephthalic acid, we demonstrate that when a thermosalient transition does not occur and a crystal polymorph has been brought to a temperature where it

DOI: 10.1021/jacs.6b07406
J. Am. Chem. Soc. 2016, 138, 13298–13306

becomes metastable, the transition can be induced by light local mechanical stimulation, whereby the crystals undergo mechanical motion. This *mechano*salient effect is initiated by local perturbation of the structure and occurs due to rapid transition and mechanical reconfiguration. Application of local pressure results in transition of macroscopic domains in the crystal and formation of multiple twins before the entire crystal is converted.

On the basis of structural and microscopic analyses, we suggest a plausible mechanism for the mechanosalient effect in terephthalic acid crystals. According to the mechanism, slanted slabs separated by slip planes which are observed as striations on the (010) face are initially transformed. These slabs rapidly change their shape, glide, and realign after gliding. The slabs play a pivotal role in the shape transformation. Because the structural difference between the two phases is small, the integrity of the crystal remains intact, and single crystals can be cycled at least 10 times between the two structures without disintegration.

The properties of terephthalic acid crystals described here resemble the "superelastic" properties of its diamide, described recently by Takamizawa and Miyamoto.[57] However, in addition to the superelastic-like behavior, the terephthalic acid crystals also exhibits self-healing and mechanosalient effect. These properties can be prescribed to the different mechanism of transition between the acid and the diamide. As shown in Figure S11, although similar infinite tapes exist in their structures, there are significant differences in the mechanism of the phase transitions between the two compounds. While the transition in the terephthalic acid can be induced by temperature and pressure and occurs by sliding of layers, the transition in terephthalamide is induced by pressure and occurs by small rotation of the rings in alternating layers, turning the sheets more corrugated. Recently, Tao and collaborators[69] reported that when the (001) face of form II crystal of CuQ_2-TCNQ is pricked by a needle, the crystals undergo remarkable changes in size and are transformed to form I, similar to earlier results on pressure-induced transitions.[67,68] The similarity in the response of these structures provides a basis to hypothesize that the mechanosalient effect could be observed with other metastable polymorphs where the stress is sufficiently high to induce motion.

4. EXPERIMENTAL SECTION

4.1. Materials. Crystalline terephthalic acid (CAS Registry No.100-21-0) was obtained from Sigma-Aldrich and used as received.

4.2. Hydrothermal Crystallization. Crystals of form I terephthalic acid were obtained from water in the presence of *p*-toluic acid at 423 K.[63] Crystals of form II were obtained by crystallization under hydrothermal conditions. The concentrations of terephthalic acid were adjusted by trials. In a typical procedure, 0.144 g of terephthalic acid was added into a 22 mL Teflon-lined stainless steel autoclave, and water acidified by acetic acid (7.2 mL of water and 0.8 mL of acetic acid) was added. The autoclave was sealed and heated at 523 K in a furnace for 3 h. After cooling down to room temperature for 6 h, the crystals were collected by filtration and dried at room temperature.

4.3. Thermal Analysis. Differential scanning calorimetry of both polymorphs was carried out on TA DSC-Q2000 instrument. Crystals were taken on a Tzero aluminum pan and heated from room temperature (298 K) to the selected temperature at rate of 10 K min^{-1}.

4.4. Single-Crystal X-ray Diffraction. Single-crystal XRD data were collected on a Bruker APEX DUO diffractometer with monochromated Mo Kα radiation (λ = 0.71069 Å) and CCD as area detector.[70] All crystallographic calculations were performed using the crystallographic software APEX 2.[70] The data were scaled and absorption correction was performed using SADABS.[71] The structures of both forms of terephthalic acid were solved by direct methods using SHELXS97[72] and refined by full-matrix least-squares methods based on F^2 using SHELXL97[72] which are embedded in the suite WinGX.[73] All non-H atoms were refined anisotropically.[74] The hydrogen atoms attached to oxygen atoms were located from the difference electron density map and refined with isotropic thermal parameters. All hydrogen atoms attached to carbon were fixed geometrically using the HFIX command in SHELX-TL.[73] The packing diagrams were generated using Mercury 3.7[75] and X-Seed,[76] and the images were rendered with POV-Ray.[77]

4.5. Microscopy. The thermomicroscopic behavior of form II terephthalic acid was observed with a hot-stage microscope (Linkam) consisting of a temperature-controlled stage THMS600-PS mounted on Q-imaging (Q32634) microscope. Crystals of form II were heated to 390 K at a constant heating rate of 8 K min^{-1}. High-speed recordings were obtained with a HotShot 1280 CC camera (NAC) mounted on a Stereozoom SMZ745T trinocular stereoscope (Nikon). A crystal of form II was placed in oil, and the heating was controlled by a thermocouple. The videos showing the transitions of form II to form I and of form I to form II were recorded at a speed of 1500 frames per second. The scanning electron microscopy (SEM) observations were carried out with a QUANTA FEG 450 electron microscope with a primary electron energy of 2−5 kV. A crystal of form II was placed in a ceramic crucible and covered with oil to record the SEM image with a steady heating rate of 5 K min^{-1} by recording one frame per second.

Atomic force microscopy (AFM) was performed on crystal of form II at room temperature using a Witec Alpha 300R Confocal Raman Microscope/AFM system in AC ("tapping") mode. Cantilever tips with a nominal tip radius smaller than 8 nm were used with a resonant frequency of ∼90 kHz. Optical images were taken with a 20× objective. The scan arrays were 50 μm × 50 or 10 μm × 10 μm, and the scan speed was ∼0.5 lines s^{-1}. Feedback control parameters were optimized for each scan. The AFM images were analyzed using Witech project software and Gwyddion,[78] and analysis consisted of tilt correction and line profile extraction. Post-treatment of the images was performed using the WSxM 4.0 Beta software.[79] A simple line-by-line flattening process was applied to the raw topography channel by excluding the height features in the image. The post-treatment resulted in removing the shadowing effects around some higher topographical features in the filtered image.

4.6. Nanoindentation. The nanoindentation measurements were performed with an Agilent G200 nanoindenter equipped with an XP head, using Berkovitch diamond indenter. Each indentation was performed using the continuous stiffness method to a depth of 1000 nm with a strain rate of 0.05, an amplitude of 2 nm, and a frequency of 45 Hz.[80] Prior to the indentation, the stiffness and the geometry of the tip were determined by using Corning 7980 silica reference sample (Nanomechanics S1495-25). In order to ensure that the tip was fully engaged, the modulus was measured between 200 and 1000 nm. The value of the Poisson's ratio was assumed to be 0.30. A comparison of the average hardness of the form II crystals of terephthalic acid (H = 0.33 ± 0.05 GPa) and the elastic modulus (E = 6.2 ± 0.7 GPa) with the relevant recent literature data[81−83] would classify this material as soft; however, in the absence of clear-cut criteria for the degree of softness of organic crystals, we were unable to definitely categorize these crystals according to their mechanical properties.

■ ASSOCIATED CONTENT

Supporting Information

The Supporting Information is available free of charge on the ACS Publications website at DOI: 10.1021/jacs.6b07406.

Optical microscopy images, thermal data, AFM images, crystallographic data, expansivity tensor plot, structure plots, nanoindentation results, and thermal expansion data, including Figures S1−S11 and Tables S1 and S2 (PDF)

DOI: 10.1021/jacs.6b07406
J. Am. Chem. Soc. 2016, 138, 13298−13306

Movie S1. Thermosalient effect in a single crystal of form II terephthalic acid heated over the phase transition, and recorded using ordinary digital camera coupled to a hot-stage microscope (AVI)
Movie S2. Hot-stage microscopy showing the shape transformation of form II to form I of a crystal which was immersed in oil and heated over the phase transition (example 1) (AVI)
Movie S3. Hot-stage microscopy showing the shape transformation of form II to form I of a crystal which was immersed in oil and heated over the phase transition (example 2) (AVI)
Movie S4. Shape transformation of form I to form II crystal restrained in oil after crystal of form I was cooled to room temperature, recorded under microscope (AVI)
Movie S5. Mechanosalient effect induced by poking of a crystal of polymorph I which has remained untransformed after cooling to room temperature, recorded using digital camera mounted on a microscope (AVI)
Movie S6. High-speed recording of the thermal transformation of a crystal, restrained in a drop of oil, from form II to form I (frame rate: 1500 s^{-1}) (AVI)
Movie S7. High-speed recording of the thermal transformation of a crystal, restrained in a drop of oil, from form I to form II (frame rate: 1500 s^{-1}) (AVI)
Movie S8. Trace of the crystal of form II transformed into form I extracted from the high-speed recording (AVI)
Movie S9. Trace of the crystal of form I transformed into form II extracted from the high-speed recording (AVI)
Movie S10. Hot-stage SEM showing the shape transformation of form II to form I (AVI)
Movie S11. High-speed recordings (1500 s^{-1}) of the mechanosalient effect. A crystal of form I is poked with a needle to induce the transformation (AVI)
Movie S12. High-speed recordings (1500 s^{-1}) of the mechanosalient effect. A crystal of form I is poked with a needle to induce the transformation (AVI)
Movie S13. High-speed recordings (1500 s^{-1}) of the mechanosalient effect. A crystal of form I is poked with a needle to induce the transformation (AVI)
Movie S14. High-speed recordings (1500 s^{-1}) of the mechanosalient effect. A crystal of form I is poked with a needle to induce the transformation (AVI)
Movie S15. High-speed recordings (1500 s^{-1}) of the mechanosalient effect. A crystal of form I is poked with a needle to induce the transformation (AVI)
Movie S16. Hot-stage microscopy showing the straightening of mechanically bent crystal of form II when it is taken over the phase transition to from I (AVI)
Movie S17. Hot-stage microscopy showing realignment of sheets in a crystal of form II which has been delaminated by applying pressure, when it is converted to form I (AVI)
Movie S18. Hot-stage microscopy showing realignment of sheets in a mechanically damaged crystal of form II upon conversion to form I (AVI)
X-ray crystallographic data for terephthalic acid form I at 390 K (CIF)
X-ray crystallographic data for terephthalic acid form I obtained by heating of form II to form I, cooling to form II and second heating to form I, recorded at 390 K (CIF)
X-ray crystallographic data for terephthalic acid form II at 290 K (CIF)
X-ray crystallographic data for terephthalic acid form II obtained by heating of form II to form I, cooling to form II, second heating to form I and second cooling to form II, recorded at 290 K (CIF)

AUTHOR INFORMATION

Corresponding Author
*pance.naumov@nyu.edu

Notes
The authors declare no competing financial interest.

ACKNOWLEDGMENTS

We thank New York University Abu Dhabi for financial support for this work. We thank Dr. Ahmad Husain for contributing to the preliminary studies. This research was partially carried out using the Core Technology Platform resources at New York University Abu Dhabi. P.N. thanks the Alexander von Humboldt foundation for the Friedrich Wilhelm Bessel Research Award.

REFERENCES

(1) Naumov, P.; Chizhik, S.; Panda, M. K.; Nath, N. K.; Boldyreva, E. V. *Chem. Rev.* **2015**, *115*, 12440−12490.
(2) Natarajan, A.; Tsai, C. K.; Khan, S. I.; McCarren, P.; Houk, K. N.; Garcia-Garibay, M. A. *J. Am. Chem. Soc.* **2007**, *129*, 9846−9847.
(3) Centore, R.; Jazbinsek, M.; Tuzi, A.; Roviello, A.; Capobianco, A.; Peluso, A. *CrystEngComm* **2012**, *14*, 2645−2653.
(4) Naumov, P.; Sahoo, S. C.; Zakharov, B. A.; Boldyreva, E. V. *Angew. Chem., Int. Ed.* **2013**, *52*, 9990−9995.
(5) Medishetty, R.; Husain, A.; Bai, Z.; Runčevski, T.; Dinnebier, R. E.; Naumov, P.; Vittal, J. J. *Angew. Chem., Int. Ed.* **2014**, *53*, 5907−5911.
(6) Medishetty, R.; Sahoo, S. C.; Mulijanto, C. E.; Naumov, P.; Vittal, J. J. *Chem. Mater.* **2015**, *27*, 1821−1829.
(7) Commins, P.; Natarajan, A.; Tsai, C.-K.; Khan, S. I.; Nath, N. K.; Naumov, P.; Garcia-Garibay, M. A. *Cryst. Growth Des.* **2015**, *15*, 1983−1990.
(8) Etter, M. C.; Siedle, A. R. *J. Am. Chem. Soc.* **1983**, *105*, 641−643.
(9) Gigg, J.; Gigg, R.; Payne, S.; Conant, R. *J. Chem. Soc., Perkin Trans. 1* **1987**, 2411−2414.
(10) Steiner, T.; Hinrichs, W.; Saenger, W.; Gigg, R. *Acta Crystallogr., Sect. B: Struct. Sci.* **1993**, *49*, 708−718.
(11) Zamir, S.; Bernstein, J.; Greenwood, D. J. *Mol. Cryst. Liq. Cryst. Sci. Technol., Sect. A* **1994**, *242*, 193−200.
(12) Lieberman, H. F.; Davey, R. J.; Newsham, D. M. T. *Chem. Mater.* **2000**, *12*, 490−494.
(13) Colombier, I.; Spagnoli, S.; Corval, A.; Baldeck, P. L.; Giraud, M.; Leaustic, A.; Yu, P.; Irie, M. *J. Chem. Phys.* **2007**, *126*, 011101.
(14) Skoko, Z.; Zamir, S.; Naumov, P.; Bernstein, J. *J. Am. Chem. Soc.* **2010**, *132*, 14191−14202.
(15) Sidelnikov, A. A.; Chizhik, S. A.; Zakharov, B. A.; Chupakhin, A. P.; Boldyreva, E. V. *CrystEngComm* **2016**, DOI: 10.1039/C6CE00840B.
(16) Sahoo, S. C.; Sinha, S. B.; Kiran, M. S. R. N.; Ramamurty, U.; Dericioglu, A. F.; Reddy, C. M.; Naumov, P. *J. Am. Chem. Soc.* **2013**, *135*, 13843−13850.
(17) Lusi, M.; Bernstein, J. *Chem. Commun.* **2013**, *49*, 9293−9295.
(18) Nath, N. K.; Panda, M. K.; Sahoo, S. C.; Naumov, P. *CrystEngComm* **2014**, *16*, 1850−1858.
(19) Panda, M. K.; Runčevski, T.; Sahoo, S. C.; Belik, A. A.; Nath, N. K.; Dinnebier, R. E.; Naumov, P. *Nat. Commun.* **2014**, *5*, 4811.
(20) Koshima, H.; Ojima, N. *Dyes Pigm.* **2012**, *92*, 798−801.
(21) Nath, N. K.; Pejov, L.; Nichols, S. M.; Hu, C.; Saleh, N.; Kahr, B.; Naumov, P. *J. Am. Chem. Soc.* **2014**, *136*, 2757−2766.

DOI: 10.1021/jacs.6b07406
J. Am. Chem. Soc. 2016, 138, 13298−13306

(22) Naumov, P.; Kowalik, J.; Solntsev, K. M.; Baldridge, A.; Moon, J.-S.; Kranz, C.; Tolbert, L. M. *J. Am. Chem. Soc.* **2010**, *132*, 5845−5857.
(23) Koshima, H.; Ojima, N.; Uchimoto, H. *J. Am. Chem. Soc.* **2009**, *131*, 6890−6891.
(24) Shima, T.; Muraoka, T.; Hoshino, N.; Akutagawa, T.; Kobayashi, Y.; Kinbara, K. *Angew. Chem., Int. Ed.* **2014**, *53*, 7173−7178.
(25) Koshima, H.; Takechi, K.; Uchimoto, H.; Shiro, M.; Hashizume, D. *Chem. Commun.* **2011**, *47*, 11423−11425.
(26) Nabetani, Y.; Takamura, H.; Hayasaka, Y.; Shimada, T.; Takagi, S.; Tachibana, H.; Masui, D.; Tong, Z.; Inoue, H. *J. Am. Chem. Soc.* **2011**, *133*, 17130−17133.
(27) Sun, J.-K.; Li, W.; Chen, C.; Ren, C.-X.; Pan, D.-M.; Zhang, J. *Angew. Chem., Int. Ed.* **2013**, *52*, 6653−6657.
(28) Guo, S.; Matsukawa, K.; Miyata, T.; Okubo, T.; Kuroda, K.; Shimojima, A. *J. Am. Chem. Soc.* **2015**, *137*, 15434−15440.
(29) Bushuyev, O. S.; Singleton, T. A.; Barrett, C. J. *Adv. Mater.* **2013**, *25*, 1796−1800.
(30) Bushuyev, O. S.; Tomberg, A.; Friščić, T.; Barrett, C. J. *J. Am. Chem. Soc.* **2013**, *135*, 12556−12559.
(31) Kobatake, S.; Takami, S.; Muto, H.; Ishikawa, T.; Irie, M. *Nature* **2007**, *446*, 778−781.
(32) Morimoto, M.; Irie, M. *J. Am. Chem. Soc.* **2010**, *132*, 14172−14178.
(33) Terao, F.; Morimoto, M.; Irie, M. *Angew. Chem., Int. Ed.* **2012**, *51*, 901−904.
(34) Uchida, K.; Sukata, S.-I.; Matsuzawa, Y.; Akazawa, M.; de Jong, J. J. D.; Katsonis, N.; Kojima, Y.; Nakamura, S.; Areephong, J.; Meetsma, A.; Feringa, B. L. *Chem. Commun.* **2008**, 326−328.
(35) Kobatake, S.; Hasegawa, H.; Miyamura, K. *Cryst. Growth Des.* **2011**, *11*, 1223−1229.
(36) Koshima, H.; Nakaya, H.; Uchimoto, H.; Ojima, N. *Chem. Lett.* **2012**, *41*, 107−109.
(37) Zhu, L.; Al-Kaysi, R. O.; Bardeen, C. J. *J. Am. Chem. Soc.* **2011**, *133*, 12569−12575.
(38) Kim, T.; Zhu, L.; Mueller, L. J.; Bardeen, C. J. *CrystEngComm* **2012**, *14*, 7792−7799.
(39) Shtukenberg, A. G.; Freudenthal, J.; Kahr, B. *J. Am. Chem. Soc.* **2010**, *132*, 9341−9349.
(40) Kitagawa, D.; Nishi, H.; Kobatake, S. *Angew. Chem., Int. Ed.* **2013**, *52*, 9320−9322.
(41) Kim, T.; Zhu, L.; Mueller, L. J.; Bardeen, C. J. *J. Am. Chem. Soc.* **2014**, *136*, 6617−6625.
(42) Kim, T.; Al-Muhanna, M. K.; Al-Suwaidan, S. D.; Al-Kaysi, R. O.; Bardeen, C. J. *Angew. Chem., Int. Ed.* **2013**, *52*, 6889−6893.
(43) Al-Kaysi, R. O.; Zhu, L.; Al-Haidar, M.; Al-Muhannah, M. K.; El-Boubbou, K.; Hamdan, T. M.; Bardeen, C. J. *CrystEngComm* **2015**, *17*, 8835−8842.
(44) Al-Kaysi, R. O.; Müller, A. M.; Bardeen, C. J. *J. Am. Chem. Soc.* **2006**, *128*, 15938−15939.
(45) Yu, Y.; Nakano, M.; Ikeda, T. *Nature* **2003**, *425*, 145−145.
(46) Zhang, L.; Liang, H.; Jacob, J.; Naumov, P. *Nat. Commun.* **2015**, *6*, 7429.
(47) Zeng, H.; Wasylczyk, P.; Parmeggiani, C.; Martella, D.; Burresi, M.; Wiersma, D. S. *Adv. Mater.* **2015**, *27*, 3883−3887.
(48) Reddy, C. M.; Krishna, G. R.; Ghosh, S. *CrystEngComm* **2010**, *12*, 2296−2314.
(49) Panda, M. K.; Ghosh, S.; Yasuda, N.; Moriwaki, T.; Mukherjee, G. D.; Reddy, C. M.; Naumov, P. *Nat. Chem.* **2015**, *7*, 65−72.
(50) Takamizawa, S.; Takasaki, Y. *Chem. Sci.* **2016**, *7*, 1527−1534.
(51) Hayashi, S.; Koizumi, T. *Angew. Chem.* **2016**, *128*, 2751−2754.
(52) Panda, M. K.; Runčevski, T.; Husain, A.; Dinnebier, R. E.; Naumov, P. *J. Am. Chem. Soc.* **2015**, *137*, 1895−1902.
(53) Islam, M. R.; Li, X.; Smyth, K.; Serpe, M. J. *Angew. Chem.* **2013**, *125*, 10520−10523.
(54) Ma, M.; Guo, L.; Anderson, D. G.; Langer, R. *Science* **2013**, *339*, 186−189.
(55) de Haan, L. T.; Verjans, J. M. N.; Broer, D. J.; Bastiaansen, C. W. M.; Schenning, A. P. H. J. *J. Am. Chem. Soc.* **2014**, *136*, 10585−10588.
(56) Takamizawa, S.; Takasaki, Y. *Angew. Chem., Int. Ed.* **2015**, *54*, 4815−4817.
(57) Takamizawa, S.; Miyamoto, Y. *Angew. Chem., Int. Ed.* **2014**, *53*, 6970−6973.
(58) Sato, O. *Nat. Chem.* **2016**, *8*, 644−656.
(59) Davey, R. J.; Maginn, S. J.; et al. *J. Chem. Soc., Faraday Trans.* **1994**, *90*, 1003−1009.
(60) Śledź, M.; Janczak, J.; Kubiak, R. *J. Mol. Struct.* **2001**, *595*, 77.
(61) Sahoo, S. C.; Panda, M. K.; Nath, N. K.; Naumov, P. *J. Am. Chem. Soc.* **2013**, *135*, 12241−12251.
(62) Ikeda, T.; Ube, T. *Nature* **2014**, *511*, 300−301. We note that, contrary to the claim in this reference that "superelasticity in a molecular crystal has been observed for the first time in a pure organic crystal", the 1994 report of Davey, Maginn and collaborators[59] reports essentially the same characteristics for terephthalic acid and appears to be the first report of a superelastic organic crystal.
(63) Bailey, M.; Brown, C. J. *Acta Crystallogr.* **1967**, *22*, 387−391.
(64) Crottaz, O.; Kubel, F.; Schmid, H. *J. Mater. Chem.* **1997**, *7*, 143−146.
(65) Nauha, E.; Lusi, M.; Naumov, P. *CrystEngComm* **2016**, *18*, 4699−4703.
(66) Cliffe, M.; Goodwin, A. *J. Appl. Crystallogr.* **2012**, *45*, 1321−1329.
(67) Jones, W.; Thomas, J. M.; Williams, J. O. *Philos. Mag.* **1975**, *32*, 1−11.
(68) Jones, W.; Williams, J. O. *J. Mater. Sci.* **1975**, *10*, 379−386.
(69) Liu, G.; Liu, J.; Liu, Y.; Tao, X. *J. Am. Chem. Soc.* **2014**, *136*, 590−593.
(70) *APEX DUO*, version 2.1-4, and *SAINT*, version 7.34A; Bruker AXS Inc.: Madison, WI, 2012.
(71) Sheldrick, G. M. *SADABS*; University of Göttingen, Göttingen, Germany, 1996.
(72) Sheldrick, G. M. *Acta Crystallogr., Sect. A: Found. Crystallogr.* **2008**, *64*, 112−122.
(73) Farrugia, L. *J. Appl. Crystallogr.* **1999**, *32*, 837−838.
(74) Sheldrick, G. M. *SHELXL-97*; University of Göttingen: Göttingen, Germany, 2008.
(75) Macrae, C. F.; Bruno, I. J.; Chisholm, J. A.; Edgington, P. R.; McCabe, P.; Pidcock, E.; Rodriguez-Monge, L.; Taylor, R.; Streek, J. V.; Wood, P. A. *J. Appl. Crystallogr.* **2008**, *41*, 466−470.
(76) Barbour, L. J. *X-Seed*, Graphical Interface to SHELX-97 and POV-Ray, Program for Better Quality of Crystallographic Figures; University of Missouri-Columbia, Columbus, MO, 1999.
(77) *POV-RAY for Windows*, Persistence of Vision; Raytracer Pty Ltd, Victoria, Australia, 2004.
(78) Nečas, D.; Klapetek, P. *Cent. Eur. J. Phys.* **2012**, *10*, 181−188.
(79) Horcas, I.; Fernandez, R.; Gomez-Rodriguez, J. M.; Colchero, J.; Gomez-Herrero, J.; Baro, A. M. *Rev. Sci. Instrum.* **2007**, *78*, 013705.
(80) Oliver, W. C.; Pharr, G. M. *J. Mater. Res.* **1992**, *7*, 1564−1583.
(81) Krishna, G. R.; Shi, L.; Bag, P. P.; Sun, C. C.; Reddy, C. M. *Cryst. Growth Des.* **2015**, *15*, 1827−1832.
(82) Krishna, G. R.; Kiran, M. S. R. N.; Fraser, C. L.; Ramamurty, U.; Reddy, C. M. *Adv. Funct. Mater.* **2013**, *23*, 1422−1430.
(83) Krishna, G. R.; Devarapalli, R.; Prusty, R.; Liu, T.; Fraser, C. L.; Ramamurty, U.; Reddy, C. M. *IUCrJ* **2015**, *2*, 611−619.

DOI: 10.1021/jacs.6b07406
J. Am. Chem. Soc. 2016, 138, 13298−13306